First 40Ar/39Ar analyses of Australasian tektites in close association with bifacially worked artifacts at Nalai site in Bose Basin, South China: The question of the early Chinese Acheulean

Véronique Michel, Xiaobo Feng, Guanjun Shen, Dominique Cauche, Marie-hélène Moncel, Sylvain Gallet, Bernard Gratuze, Jiang Wei, Xiaorong Ma, Kangti Liu

First 40Ar/39Ar analyses of Australasian tektites in close association with bifacially worked artifacts at Nalai site in Bose Basin, South China: The question of the early Chinese Acheulean

Véronique Michel, Xiaobo Feng, Guanjun Shen, Dominique Cauche, Marie-hélène Moncel, Sylvain Gallet, Bernard Gratuze, Jiang Wei, Xiaorong Ma, Kangti Liu

First $^{40}Ar/^{39}Ar$ analyses of Australasian tektites in close association with bifacially worked artifacts at Nalai site in Bose Basin, South China: the question of the early Chinese Acheulean

Véronique Michel[a, b, *]

veronique.michel@cepam.cnrs.fr

Xiaobo Feng[c]

Guanjun Shen[d]

Dominique Cauche[e]

Marie-Hélène Moncel[f]

Sylvain Gallet[b]

Bernard Gratuze[g]

Jiang Wei[h]

Xiaorong Ma[i]

Kangti Liu[i]

[a]Université Côte d'Azur, CNRS, CEPAM, 06300, Nice, France

[b]Université Côte d'Azur, CNRS, Observatoire de la Côte d'Azur, IRD, Géoazur, 06560, Valbonne, France

[c]College of Applied Arts and Science, Beijing Union University, Beijing, 100191, China

[d]College of Geographical Sciences, Nanjing Normal University, Nanjing, Jiangsu, 210023, China

[e]Institut de Paléontologie Humaine, HNHP CNRS-MNHN, 75013, Paris, France

[f]UMR 7194 HNHP (MNHN-CNRS-UPVD), Département Homme et Environnement, Muséum National d'Histoire Naturelle, 75013, Paris, France

[g]UMR 5060, IRAMAT, CNRS-Université d'Orleans, Centre Ernest-Babelon, 45071, Orleans, France

[h]Museum of Guangxi, Zhuang Autonomous Region, 530022, Nanning, China

[i]Youjiang Museum of Nationalities, 533000, Bose, China

[*]Corresponding author.

Abstract

The recently discovered Nalai site is one of the Bose Basin localities, which is key to studying the earliest bifaces in China. The Nalai site has yielded an abundance of lithic artifacts, including bifaces and tektites in close association. The total fusion $^{40}Ar/^{39}Ar$ method was applied to four tektites discovered beside and contemporaneous with bifaces in the red laterite sediments of the upper levels of the T4 terrace (layers 4 and 5). Our $^{40}Ar/^{39}Ar$ data with a weighted mean age of 809 ± 12 ka provide for the first time unequivocal dates for bifacial production at Bose, broadly consistent with the precise Australasian tektite age of 788.1 ± 2.8 ka, recently published by Jourdan et al. (2019). The relatively important errors reported here suggest sample contamination by clasts or bubbles for the oldest aliquots and alteration for the younger ones. The lithic assemblage from

layers 4 and 5 of the Nalai site is quite similar to that found at other sites in the Bose Basin. The assemblages are dominated by choppers, but bifaces, picks, and unifaces give a Mode 2 and Acheulean-type character to the series. The high frequency of the round tongue-shaped tip, a low elongation index, and a wide and thick base characterize the lLarge eCutting tTools. These results contribute to resolving ongoing debates on the timing and origin of bifaces and the Acheulean in China.

Keywords: Lower paleolithic; Argon dating; Total fusion; LCT assemblage; Mode 2; Fourth terrace T4

1 Introduction

The Acheulean is considered a cognitive and technological threshold in human evolution (e.g., Semaw et al., 2009; Lepre et al., 2011; Beyene et al., 2013; de la Torre, 2016; Moncel and Ashton, 2018). Many questions still surround the dispersal of this technology in Eurasia and especially in China. In the current state of knowledge, biface production, and more generally the ability to make lLarge eCutting tTools (LCTs, i.e., bifaces, cleavers, picks), appeared in East Africa from 1.76 to 1.2 Ma onward (e.g., Semaw et al., 2009; Lepre et al., 2011; Beyene et al., 2013; de la Torre, 2011, 2016; de la Torre et al., 2008; de la Torre and Mora, 2018). In the Levant, an early 'oOut-of-Africa' dispersal is dated from 1.6 to 1.2 Ma, and a second one is recorded at around 800 ka at 'Ubeidiya and Gesher Benot Yak'ov sites, in Israel (Bar-Yosef and Goren-Inbar, 1993; Martinez-Navarro et al., 2012; Goren-Inbar et al., 2018). In Western Europe, the Acheulean occurs later, from 700 ka onward, and perhaps intermittently at 900 ka (Moncel et al., 2013; Vallverdu et al., 2014; Voinchet et al., 2015; Moncel and Ashton, 2018).

For Asia, the timing and origin of the Chinese assemblages with bifaces (or ~~hand axes~~handaxes (Please it is handaxes not hand axes for all the MS)) are still controversial. Following Hou et al. (2000), the age of the earliest bifaces in China and the close association between tektites and bifaces have not yet been demonstrated (e.g., Koeberl and Glass, 2000). A solid chronological framework however is essential for discussing the timing and origin of biface production in China. Assemblages in India (from 1.5 Ma) and southeastern insular Asia (800 ka, Indonesia) are considered to be Acheulean dispersals from the Levant of the Large Flake Acheulean tradition (LFA) (Sharon, 2007; Pappu et al., 2011). Chinese bifaces were first discovered in the 1930s, but particularly from the 1970s onward (Hou et al., 2000), fueling discussions of the famous Movius Line dividing areas with ~~hand axes~~handaxes from areas with pebble tools (Movius, 1944; Lycett and Bae, 2010). New discoveries of lithic assemblages with bifaces cast doubt on the reality of the Movius Line (i.e., Wang et al., 2012).

Currently, series with bifaces are found in several areas in China, including the sites of Dingcun, Bose, and Luonan (Li et al., 2018). Two hypotheses have been proposed to define relationships between China, Africa, and the Levant: (1) a local onset in China derived from previous core-and-flake assemblages (convergence) and (2) early and external arrivals attested by common features with the African Acheulean (Hou et al., 2000; Zhang et al., 2010; Huang et al., 2012; Wang et al., 2012; Xu et al., 2012; Kuman et al., 2014, 2016; Li et al., 2014, 2016, ~~2017,~~ 2018; Wang and Bae, 2015; Li et al., 2017; (Li et al., 2017 are not the same author as Li et al., 2014, 2016, 2018)Sherwood et al., 2018; Guan et al., 2018; Lei et al., 2020). Consequently, the direct dating of tektites found in close association with bifaces is the best way to improve and verify the dating of the earliest bifaces yet known in China. New excavation evidence offers the opportunity to discuss the context of the bifaces in China, which has been an ongoing source of debate for the past two decades, as well as the emergence of biface production in China and relationships to the Acheulean tradition (e.g., Langbroek, 2015; Wang and Bae, 2015).

In southeastern Asian and Antarctic regions, including the South of China, tektites and microtektites have been discovered and dated to around 780–800 ka (Hou et al., 2000; Folco et al., 2011; Jourdan et al., 2019). Tektites are natural K-bearing glass produced by the fusion of the upper continental crust during meteorite impact. Such impact leads to the formation of an impact structure, and tektites are found at varying distances from it. The strewn field of Australasian microtektites/tektites covers vast regions of Asia, Australia, and the Antarctic (Glass and Koeberl, 2006; Mizera et al., 2016; Folco et al., 2010; Schwarz et al., 2016; Jourdan et al., 2019), with a source impact location in an area centered over Southeast Asia (~~Cavosie et al., 2017~~Cavosie et al., 2018), possibly in Indochina (Rochette et al., 2018) or in Southern Laos (Sieh et al., 2020).

More than a hundred Paleolithic sites have been identified in the Bose Basin in Southern China (Huang et al., 2012). The Bose Basin is about 80 km in length and about 15 km in width, with seven river terraces (Wang et al., 2014). The prehistoric sites are located on the fourth terrace (T4) of the Youjiang River, Guangxi Zhuang Autonomous Region (Xie and Bodin, 2007). Tektites were discovered in the red laterized upper levels (5- to 10-m thick) (Huang et al., 2012), where artifacts were found during excavations. The tektites from the Bose Basin were first dated by fission tracks (Guo et al., 1997). The authors obtained an age of 732 ± 39 ka on tektites from the Bogu (Baigu) site. The $^{40}Ar/^{39}Ar$ method was then applied to two tektites from the Bogu site and one from the Yangwu site (Hou et al., 2000). The authors obtained an overall weighted mean age of 803 ± 3 ka (1σ) from the isochron ages of three samples (Hou et al., 2000; Potts et al., 2000). Recently, Jourdan et al. (2019) dated four Australasian tektites with high precision: from Southern China (Hou et al., 2000), Western Australia, Thailand, and Vietnam. Age plateau and isochron diagrams yielded a very precise age of 788.1 ± 2.8 for these Australasian tektites, including the recent $^{40}Ar/^{39}Ar$ age of 793 ± 14 ka proposed by Schwarz et al. (2016).

In this study, we conducted analyses of tektites from the prehistoric site of Nalai, discovered in 2003, covering an area of 30,000 m^2 and located 5 km to the southwest of the county town of Tianyang, on the fourth terrace (T4) of the right bank of the Youjiang River (Xie and Bodin, 2007; Gao, 2012; Liao et al., 2017, Fig. 1). More than 3000 artifacts were recovered, including bifacial tools and more than 300 tektites. Some bifaces were discovered in close association with tektites (Fig. 2), providing the opportunity for clear and unequivocal dating of the emergence of the Acheulean culture in China.

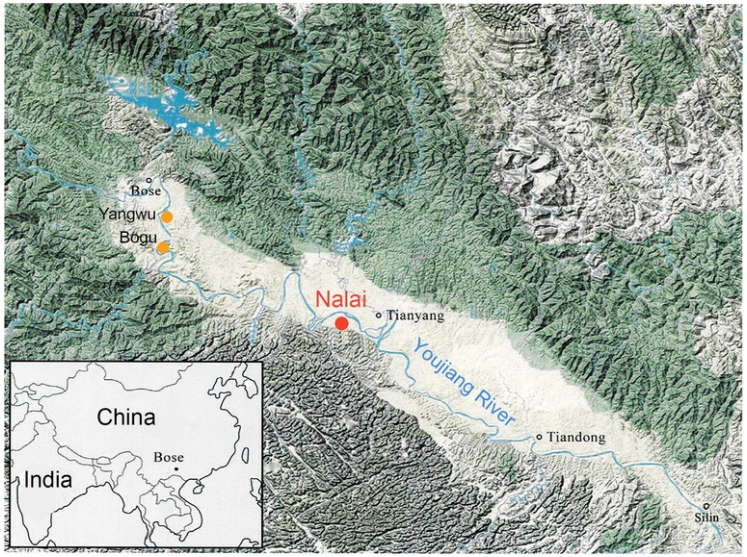

Figure 1 Location of Nalai site in the Middle Bose Basin. Bogu and Yangwu sites in the Western Bose Basin were dated using the $^{40}Ar/^{39}Ar$ method after Hou et al. (2000). Map after Wang et al. (2014) with modifications.

alt-text: Figure 1

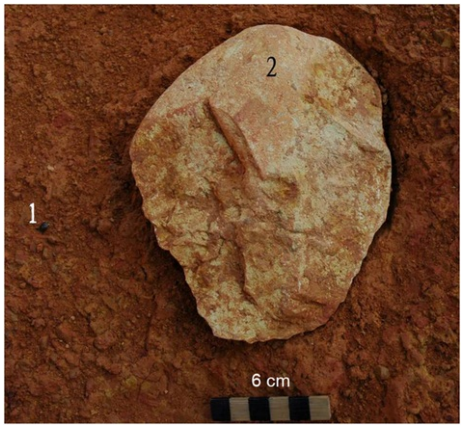

Figure 2 A photograph showing the in situ discovery of the biface N790 (2) in close association with the tektite N795 (1), at the interface between layers 4 and 5 in the excavation square NT2, considered to belong to ~~layer 5 in~~ layer 5 (Table 1) and described in the text.

alt-text: Figure 2

1.1 Nalai geography and stratigraphy

The site is located in Nalai village (N23°43′ 27″, E106°51′ 42″), 155.7 m above sea level (abs), following Liao et al. (2017; Supplementary Online Material [SOM] Fig. S1). In 2005 and 2006, an excavation of 4000 m^2 was carried out by the Guangxi Institute of Cultural Relics Protection and Archaeology. A total of nine stratigraphic layers were identified from top to bottom in square SAT16 (Fig. 3), wherein stratigraphy is well defined and similar to other squares (Fig. 4). Eight layers can be grouped into two units: the upper unit and the lower unit. The upper unit includes layers 1–3, and the lower unit comprises layers 4–8. Based on the comparative study of stratigraphy and chronology with other sites in the Bose Basin, together with the characteristics of the cultural remains, layers 1–2 belong to the Holocene, layer 3 belongs to the late Pleistocene, and layers 4–8 belong to the early Pleistocene (about 800 ka).

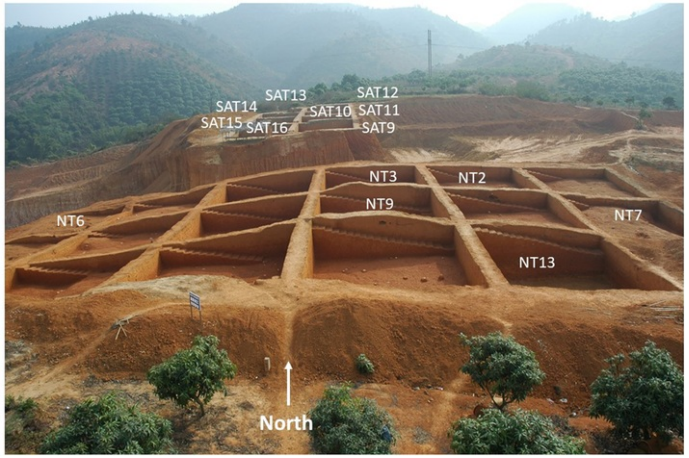

Figure 3 Photograph of Nalai site with location of squares where artifacts and tektites presented and analyzed in the text were recovered (squares TN EA T15, T16, and T19 are out of range of this photograph). Information regarding scale: SAT1–SAT8 squares are 5 m × 5 m, and all others are 10 m × 10 m.

alt-text: Figure 3

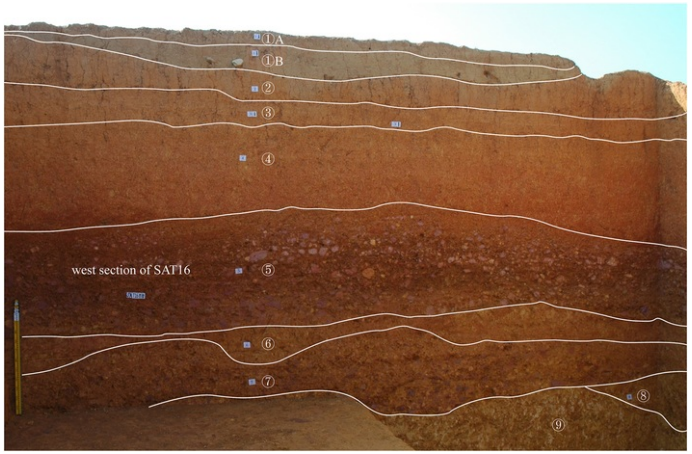

Figure 4 West section of square SAT16 with 9 layers (the stratigraphy of this square is the same for the whole site): layer 1, loam disturbed by farming, gray brownish in color; layers 2 and 3, slightly compact, yellowish layers, with ground stone implements and a few stone artifacts layer 4, mottled laterite, hard and compact, with stone artifacts such as choppers and scrapers with the presence of tektites; layer 5, a purple sandstone lump conglomerate layer. Stone artifacts comprising hand axes and picks were found in this layer. Tektites were also found in association with hand axes and picks; layers 6–8 are laterites, containing a few iron-manganese concretions. Some stone artifacts were found in these layers; layer 9 is a basal gravel layer. (For interpretation of the references to colour in this figure legend, the reader is referred to th Web version of this article.)

alt-text: Figure 4

Of a total of about 300 tektites found in Nalai site, 116 have been recovered from squares SAT1 to SAT16 and come from the interface between layers 4 and 5 (Figs. 3–4). Most of the remaining tektites from the square of other areas come also from the interface between layers 4 and 5, but in these areas, there a few tektites scattered at different depths of layer 4.

1.2 Lithic assemblage

During the 2005–2006 excavations, the Nalai site yielded an abundant lithic industry with a total of 1618 artifacts found in stratigraphy in layers 4 and 5 (Table 1), associated with more than 300 Australasian tektites. As for all

the other sites in the Bose Basin, located at the same level of the T4 river terrace, no fossil faunal remains are associated with the artifacts and tektites owing to chemical alteration of the sediments transformed into laterite.

Table 1 Industry from layer 4 and layer 5 of Nalai site, Bose Basin.

alt-text: Table 1

Type	Layer 4	Layer 5	Number	%
Whole and broken pebble	115	329	444	27.44
Hammerstone	5	14	19	1.17
Single scar chopper	17	19	36	2.23
Chopper	80	139	219	13.53
Chopping tool	4	27	31	1.92
Biface	0	14	14	0.87
Pick	4	27	31	1.92
Uniface	0	2	2	0.12
Core	57	65	122	7.54
Flake	75	78	153	9.45
Debris	190	326	516	31.89
Small retouched tool	9	22	31	1.92
Total	556	1062	1618	100

The Nalai tool kit is characterized by a dominant LCT assemblage, with mainly choppers and a few chopping tools (Fig. 5, no. 7–9; Fig. 6, no. 3–7) and some picks, bifaces, and unifaces (Figs. 2 and 5, no. 1–6; Fig. 6, no. 1–2). There are no spheroids or cleavers. Nineteen hammerstones were identified among the pebbles, bearing percussion tracks. The lithic raw materials are locally available river pebbles, mainly sandstone (38.7%) and limestone (32.3%), secondary siltite (9.7%) and quartz (9.7%), and also quartzite (3.2%), silicified limestone (3.2%), and volcanic rocks (3.2%).

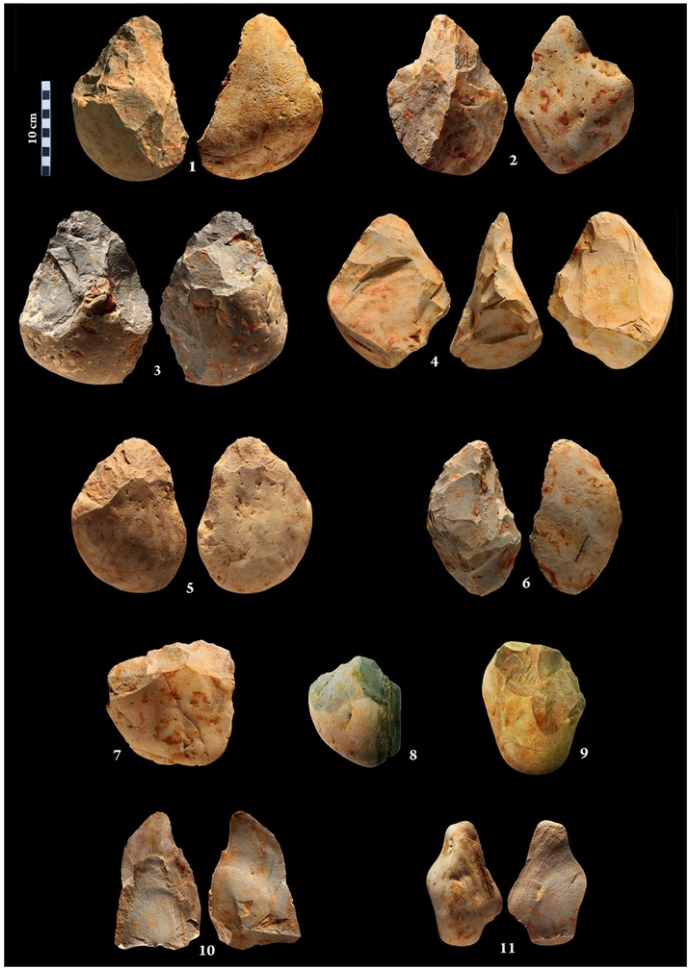

Figure 5 Lithic artifacts from layers 4 and 5 of Nalai site: 1, tongue-shaped pick (N1161, square SAT13, layer 5); 2, pick (N1175, square SAT12, layer 5); 3 and 4, tongue-shaped hand axes (3: N975, square SAT13, layer interface 4/5; 4: N842, square SAT10, layer interface 4/5); 5, partial tongue-shaped ~~hand ax~~handaxe (N1608, square SAT14, layer 5); 6, uniface (N1482, square SAT9, layer 5); 7–9, choppers (7: N808, square SAT16, layer interface 4/5; 8: N137, square TN EA T15, layer 5; 9: N112, square TN EA T19, layer 5); 10, large semi-cortical flake (N806 square SAT16, layer interface 4/5); 11, large cortical flake (N970, square SAT3, layer interface 4/5). Layer interface 4/5, corresponding to the bottom of layer 4 and to the surface of layer 5, is considered to belong to layer 5 ~~in~~(Table 1) and described in the text.

alt-text: Figure 5

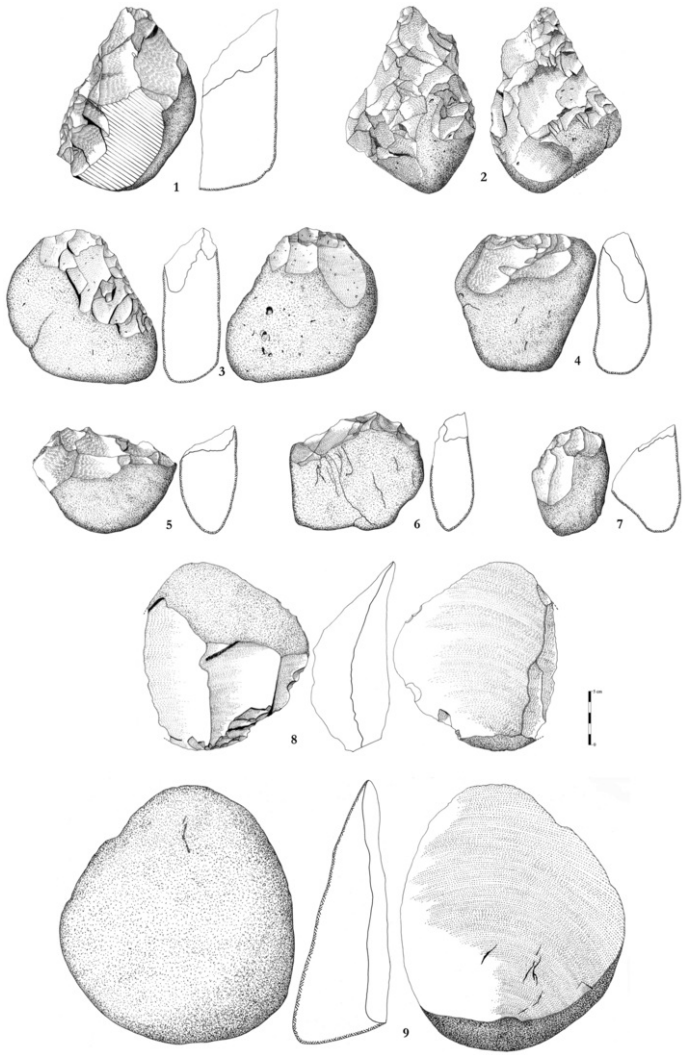

Figure 6 Drawings of lithic artifacts from layers 4 and 5 of Nalai site: 1, pick (N1647, square SAT11, layer 4); 2, ~~hand ax~~handaxe (N360, square NT7, layer interface 4/5); 3, bifacial chopper (N1293, square SAT15, layer 5); 4–7, choppers (4: N135, square TN EA T16, layer 5; 5: N113, square NT3, layer 4; 6: N184, square NT9, layer 4; 7: N152, square NT6, layer 4/5); 8, large semi-cortical flake (N711, square SAT14, layer 4); 9, very large cortical flake (N346, square SAT3, layer 4).

alt-text: Figure 6

1.3 Large cutting tools

The most frequent heavy-duty tools are choppers (unifacial pebble tools). They are shaped on pebbles and measure on average 121 × 120.4 × 53.8 mm for an average weight of 0.94 kg. More rarely, some pebbles bear a single flake removal ($n = 36$), and some choppers with bifacial flake removals are present ($n = 31$; chopping tool, Fig. 6, no. 3).

Some bifaces, picks, and unifaces are associated with the pebble tools. We designate as uniface pieces with flake removals covering only one face. Conversely, for bifaces, shaping is bifacial even if few flake removals are observed on one face while the opposite face is intensively shaped. Pieces with dense shaping on one face and few flake removals on the opposite cortical face are considered partial bifaces or bifacially worked tools. They represent a small proportion of the lithic material and LCTs, but nonetheless give a Mode 2 (and Acheulean-type) character to the assemblage (Figs. 2 and 5, no. 1–6; Fig. 6, no. 1–2). Layers 4 and 5 contain a total of 14 bifaces, 31 picks, and two

unifaces. Unlike for choppers, larger pebbles were collected for making bifaces, picks, and unifaces. They display average dimensions of 180.1 × 130.1 × 77.9 mm for an average weight of 1.7 kg. For the 14 bifaces, the average size is 176.7 × 140 × 88.5 mm for an average weight of 1.896 kg. Among the series, 12 have a round-shaped tip, with more or less concave edges, often with a wide and thick base. The elongation index (width/length) is low: 0.801. The bifaces are shaped on pebbles of various morphologies (flat, thick oval, thick cubic), most often with a first series of deep and often invasive flake removals, leaving a large part of the proximal part of the tool cortical. Frequently, a second sequence of shorter and semiabrupt flake removals covers the edges and especially the tip of the tool, which is mostly lingual, rounded, and very thin in contrast to the base of the tool. This tip is carefully shaped, often regularized by retouching, and possibly constitutes the active functional part of the tool, opposite the thick and wide cortical base corresponding to the prehensile part.

Only 26 of the 31 picks were analyzed as the others were not sufficiently well preserved. They measure on average 187.2 × 125.7 × 78.7 mm for an average weight of 1.79 kg, and 15 of them are ~~tongue~~ (tongue shaped is correct) ~~shaped~~, as are many of the bifaces. This morphofunctional characteristic does not depend on the unifacial or bifacial shaping process. The picks, on average, are shorter than the bifaces, with an elongation index of 0.726 ($n = 26$). Picks are shaped on thick, sometimes quadrangular, pebbles, and management differs on the two converging edges. One of the edges can be shaped over a larger area than the opposite edge (see Fig. 5, no. 1 and Fig. 6, no. 1). These tools bear two series of flake removals: the first with large and deep flake removals and the second with shorter and semiabrupt flake removals. These can be followed by a final phase of regularization of the edges by thick retouching, especially at the tip, which in more than half of the cases is a lingual tip, as is the case for many of the bifaces in the area. Otherwise, the tip may be a short rectilinear and transverse edge or a point with a trihedral cross section. A large part of the cortical surface is maintained at the base and on more than half of one or two edges.

The two unifaces measure 176 × 109 × 44.5 mm and have an average weight of 0.925 kg. They are also round-shaped (round shaped is correct), and the elongation index is 0.618. One of the unifaces is tongue-shaped (tongue shaped is correct), the other is half-moon-shaped (half-moon shaped is correct) (Fig. 5, no. 6). Shaping entirely covers one of the faces, starting with large invasive flake removals, followed by several series of short and oblique flake removals (flake removals is correct). The edges are regularized by retouching. The tip is rounded or lingual, and macrotraces of use are visible by direct and inverse scars.

1.4 Core technologies

LCTs are the main component of this lithic assemblage, but core technology is also present on the site, as shown by numerous cores, debris, and flakes (Fig. 5, no. 10–11; Fig. 6, no. 8–9). Three categories of cores can be defined: (1) cores with a single platform and one knapping surface (80%), (2) cores with two striking platforms and two or three flaking surfaces, and (3) a few cores with multiple striking platforms. They mainly measure more than 150-mm long. Striking platforms are generally cortical and not prepared, and debitage takes advantage of the natural form of the pebbles. The number of flake removals (flake removals is correct) is low, and the cores are not exhausted (Xie and Bodin, 2007). Some flakes are large, measuring more than 10-cm long (13%; Fig. 5, no. 10–11; Fig. 6, no. 8); some are very large, measuring more than 20-cm long (Fig. 6, no. 9). Debitage was most often performed by direct freehand percussion, but the very large, massive, and cortical flake in sandstone N364 (Fig. 6, no. 9), measuring 254 × 218 × 81 mm and weighing 4.1 kg, was obtained by launched percussion against a passive hammer. The flakes are mainly raw materials, the result of core reduction, and also by-products of the shaping of LCTs. Cortical and semicortical flakes dominate the series. Butts are mainly cortical (60%), in keeping with observations of the cores. Several refits of artifacts in layers 4 and 5 (including flakes) attest to the good preservation of the material in situ and demonstrate the in situ production of artifacts. Light-duty tools are rare ($n = 31$), represented by some crudely retouched flakes.

The lithic assemblage of layers 4 and 5 of the Nalai site is quite similar to that found at other sites in the Bose Basin and associated with tektites (Hou et al., 2000; Xie and Bodin 2007; Zhang et al., 2010; Huang et al., 2012; Wang et al., 2014; Liao et al., 2017; Feng et al., 2018). The assemblages are all dominated by choppers. Bifaces, picks, and unifaces are much rarer and are characterized by the high frequency of the tongue-shaped tip, a low elongation index, and a wide and thick base.

2 Materials and methods

Four tektites (N411, N425, N862, and N959) were extracted from the fluvial terrace of the Nalai site and analyzed using the $^{40}Ar/^{39}Ar$ method (Fig. 7). The tektites (~0.2–0.6 g) show no signs of fluvial abrasion, they are very angular and sharp, and therefore, they were not redeposited by a river. Tektite samples were cleaned in an ultrasonic water bath to remove surface-bonded residues (Fig. 7), then reduced to pieces, some of which were further crushed in an agate mortar and separated into subsamples for multiple analyses. Each analysis is a total fusion (TF) of approximately 10–15 mg of tektite per subsample. The samples were irradiated for 24 min in the nuclear reactor at McMaster University (Hamilton, Canada) with cadmium shielding position 5C (i.e., in the flux area and receiving flux from all directions) and stored for one month in the laboratory. Cadmium shielding lowers undesirable interferences during neutron irradiation and is commonly used for ‘young samples’ (i.e., Quaternary samples; Tetley and McDougall, 1980; Renne et al., 2008; McDougall, 2014). The samples then were placed in the cavities of a copper plate for mass spectrometer analysis (VG 3600 with a Daly detector; Fig. 8A). $^{40}Ar/^{39}Ar$ geochronology was performed at the Géoazur Laboratory with detailed parameters listed in SOM, as in Jourdan et al. (2006) and Michel et al. (2013).

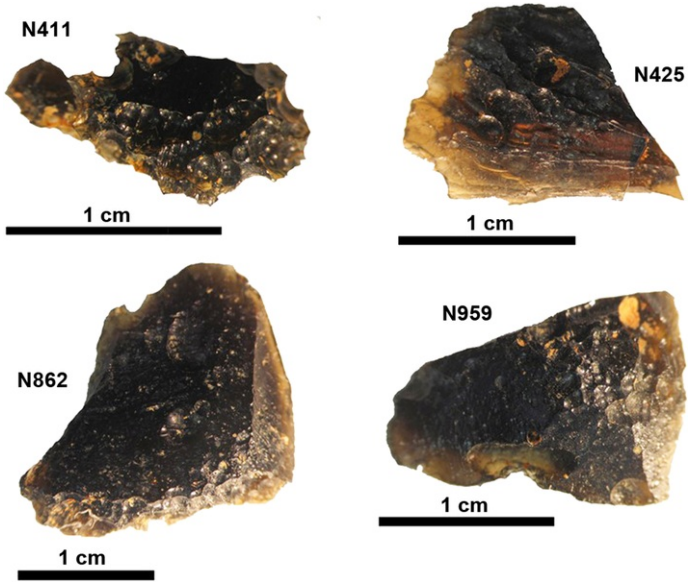

Figure 7 Four tektites from layers 4 and 5 of Nalai site, analyzed using the $^{40}Ar/^{39}Ar$ method: N411 (upper left; square NT13, Z = 155 cm, layer interface 4/5), N425 (upper right; NT13, Z = 110 cm, layer interface 4/5), N862 (lower left; SAT10, Z = 220 cm, layer interface 4/5), N959 (lower right; SAT13, Z = 265 cm, layer 4).

alt-text: Figure 7

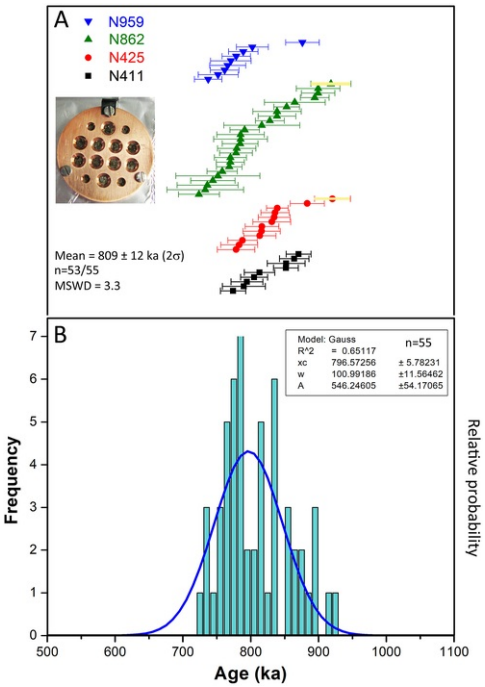

Figure 8 (A) Tektites were ground and loaded as subsamples of about 10 mg onto a copper plate for total fusion (TF). Distribution of $^{40}Ar/^{39}Ar$ ages at 2σ by TF of each subsample for tektites N959, N862, N425, and N411 (Table 2). Blue symbols are N959 TF

ages, green symbols are N862 TF ages, red symbols are N425 TF ages, and black symbols are N411 TF ages. Fifty-three of the 55 dates yield a weighted average of 809 ± 12 ka using Isoplot version 3.0 software (Ludwig, 2003). The two yellow bars are outlie data. (B) Frequency histogram of the TF $^{40}Ar/^{39}Ar$ ages (n = 55) shows a normal distribution yielding to a Gauss function adjusted using Origin version 2016 Sr2 software. The probability density distribution is centered at 796.6 ± 5.7 ka with a coefficient (r^2) of 0.65. MSWD = mean square of weighted deviates. (For interpretation of the references to colour in this figure legend, the reader is referred to the Web version of this article.)

alt-text: Figure 8

Each subsample was fused with a CO_2 laser, and the evolved gas was purified in a stainless steel and glass extraction line fitted with two Al-Zr getter pumps (working at 450 °C and room temperature, respectively) and a liquid nitrogen trap. The spectrometer sensitivity is, on average, 2.0 E-14 mol/V. Background values were constrained by measuring blanks for every two or three analyzed samples. Mass discrimination was monitored by regularly analyzing one air pipette volume. The ultimate accuracy of the $^{40}Ar/^{39}Ar$ method depends on well-dated homogeneous standards (Kuiper et al., 2008; Renne et al., 2009). The $^{40}Ar/^{39}Ar$ technique yields ages referenced back to a mineral standard of known age. Mineral standards (i.e., Alder Creek sanidine) of known age are necessary to determine the neutron dose (J value) of a sample to be able to calculate the $^{40}Ar/^{39}Ar$ age of an unknown sample (Jourdan et al., 2014). J values were calculated using an age of 1.194 ± 0.004 Ma (Nomade et al., 2005) for Alder Creek sanidine and the total decay constant of Steiger and Jäger (1977). The composition of major elements was determined for the four dated tektites by ~~l~~Laser ~~a~~Ablation ~~i~~Inductively ~~c~~Coupled ~~p~~Plasma ~~m~~Mass ~~s~~Spectrometry (LA-ICP-MS) (see additional details in SOM S1).

3 Results

The major element composition obtained for the dated tektite N411, N425, N862, and N959 is given in SOM Table S1. The ranges for the major element composition are as follows: SiO_2 = 70.31–71.76 wt. %, Al_2O_3 = 14.61–15.58 wt. %, Fe_2O_3 = 4.99–5.35 wt. %, CaO = 2.43–2.65 wt. %, K_2O = 2.10–2.25 wt. %, MgO = 2.07–2.19 wt. %, TiO_2 = 0.68–0.70 wt. %, P_2O_5 = 0.05–0.06 wt.%, and MnO = 0.094–0.099 wt. %. The major composition clearly places the Nalai tektites in the group of strewn field Australasian tektites after Koeberl (1990), Heide et al. (2001), Glass and Koeberl (2006), and Schwarz et al. (2016) data.

The $^{40}Ar/^{39}Ar$ analytical results of tektites N411, N425, N862, and N959 are presented in SOM Tables S2, S3, S4, and S5, respectively, and the determined ages are summarized in Table 2. TF of nine subsamples was carried out for the tektite N411, which gave a mean age range of between 774 and 852 ka (SOM Table S2), while 12 subsamples of N425, 24 subsamples of N862, and 10 subsamples of N959 gave $^{40}Ar/^{39}Ar$ ages in the mean range of 778–920 ka (SOM Table S3), 723–918 ka (SOM Table S4), and 737–876 ka (SOM Table S5), respectively. The weighted mean age, using Isoplot version 3.0 software (Ludwig, 2003), is 809 ± 12 ka (2σ; n = 53/55, mean square of weighted deviates [MSWD] = 3.3; Fig. 8A). All dates yield an age distribution displayed by Gaussian probability density centered at 797 ± 6 ka, using Origin version 2016 Sr2 software (OriginLab Corporation, Northampton; Fig. 8B).

Table 2 $^{40}Ar/^{39}Ar$ ages from total fusion of N411, N425, N862, and N959 tektites with ages using Isoplot and Origin software and corresponding inverse isochron ages, trapped argon composition $(^{40}Ar/^{36}Ar)_0$, and MSWD.[a-b]

alt-text: Table 2

Total fusion									
N411		N425		N862		N862		N959	
Age (ka)	±2σ	Age (ka)	±2σ	Age (ka)	±2σ	Age (ka)	±2σ	Age (ka)	±2σ
851.5	36.7	813.1	47.5	864.6	89.7	751.2	124.1	777.9	47.9
804.6	39.6	920.2	53.0	852.6	37.8	894.0	42.3	765.6	53.0
773.5	37.2	883.1	50.4	899.1	64.4	743.8	65.3	751.6	58.9
863.7	43.3	816.1	49.5	723.3	60.6	784.0	52.9	802.0	46.7
812.6	44.8	782.5	54.4	732.5	113.0	735.8	89.7	788.6	43.6
870.3	36.5	778.0	54.9	815.9	112.0	779.0	56.4	736.9	40.5
851.9	55.7	834.2	46.8	838.5	71.3	767.9	37.5	761.1	41.9
794.1	47.0	835.5	41.9	838.4	55.6	757.6	44.5	875.9	49.7
789.4	63.3	815.6	55.2	917.9	59.3	769.6	47.0	778.2	41.7
		830.7	55.8	827.8	42.5	790.7	43.4	770.4	59.8

		787.5	43.5	784.6	79.4	769.5	41.4		
		838.9	31.7	899.0	49.3	784.6	70.0		
Isoplot	Mean ± 2σ		809 ± 12 ka		MSWD = 3.3				
Origin	Gauss center ± 2σ		796.6 ± 6 ka		r^2 = 0.65				
Inverse isochron		N411		N425		N862		N959	
Age (ka) ± 2σ		845.0 ± 43.7		836.5 ± 40.8		813.0 ± 29.6		772.8 ± 51.4	
$(^{40}Ar/^{36}Ar)_0$ ± 2σ		283.0 ± 38.6		288.2 ± 31.6		297.3 ± 22.7		304.8 ± 46.8	
MSWD		3.41		1.68		4.52		2.87	

[a] Ages determined using Isoplot version 3.0 and Origin version 2016 Sr2.

[b] MSWD = mean square of weighted deviates.

The measurement of ^{36}Ar in $^{40}Ar/^{39}Ar$ dating allows for plotting the inverse isochron graph. The results are a series of data points ranging from pure atmospheric argon to pure radiogenic argon. A regression line through these data points forms an inverse isochron, and the point at which the isochron intercepts with the x-axis yields the $^{39}Ar/^{40}Ar^*$ of the samples and therefore the age (Table 2). For the tektite N411 (SOM Table S2), the data points plot linearly, yielding an intercept age of 845.0 ± 43.7 ka (2σ) and a trapped argon composition $(^{40}Ar/^{36}Ar)_0$ of 283.0 ± 38.6 (2σ), with a MSWD of 3.41 (Fig. 9). Similarly, for the tektite N425 (SOM Table S3), data yield an age of 836.5 ± 40.8 ka (2σ), with a $(^{40}Ar/^{36}Ar)_0$ of 288.2 ± 31.6 (2σ) and with a MSWD of 1.68. For the tektite N862 (SOM Table S4), the intercept age is 813.0 ± 29.6 ka (2σ), with a $(^{40}Ar/^{36}Ar)_0$ of 297.3 ± 22.7 (2σ) and a MSWD of 4.52. For the tektite N959 (SOM Table S5), the intercept age is 772.8 ± 51.4 (2σ), with a $(^{40}Ar/^{36}Ar)_0$ of 304.8 ± 46.8 (2σ) and with a MSWD of 2.87. All initial ratios $(^{40}Ar/^{36}Ar)_0$ are in agreement with each other, and the current atmospheric composition is within ± 2σ (298.56 ± 0.31; Lee et al., 2006). All isochron graphs yield high MSWD (>1), which indicate dispersive data and suggest the presence of inherited Ar owing to clasts or bubbles for the oldest aliquots and alteration for the youngest ones. Therefore, our $^{40}Ar/^{39}Ar$ results can be used as dating markers with apparent TF ages ranging from 774 ka to 920 ka, with a weighted mean age of 809 ± 12 ka, consistent with the error range of the precise Australasian tektite age of 788.1 ± 2.8 ka (Jourdan et al., 2019). Thus, an age of about 800 ka can be attributed to these tektites. The important errors obtained here (2σ), compared with those of Hou et al. (2000), may possibly be related to the fact that this is an average from a TF series, whereas Hou et al. (2000) reached plateau ages (5–13 steps) in temperature increments and achieved corresponding isochron ages.

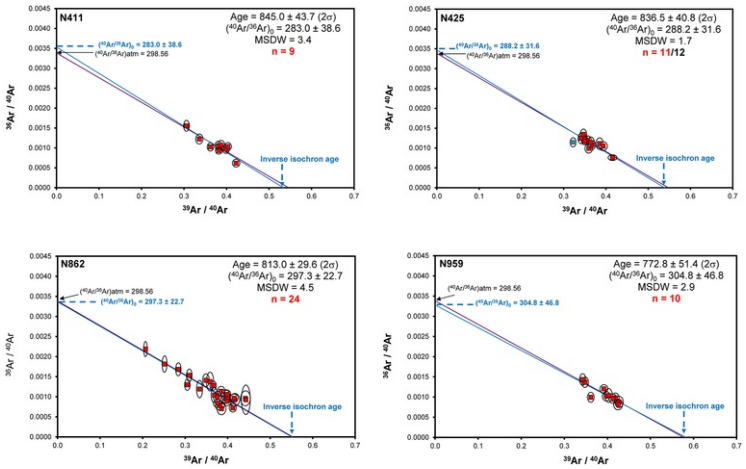

Figure 9 $^{36}Ar/^{40}Ar$ vs. $^{39}Ar/^{40}Ar$ inverse isochron diagram for all the data of tektites N411 (upper left), N425 (upper right), N862 (lower left), and N959 (lower right) and $^{40}Ar/^{39}Ar$ age at the intercept, with the x-axis yielding to the $^{39}Ar/^{40}Ar^*$ of the sample. A regression line through data points forms an inverse isochron, and the intercept with the x-axis yields the $^{39}Ar/^{40}Ar^*$ of the samples and therefore the age. MSWD = mean square of weighted deviates.

alt-text: Figure 9

4 Discussion and conclusion

The $^{40}Ar/^{39}Ar$ dating results presented here, on four tektites from the Nalai site found in situ in close association with bifaces, show that the upper laterite levels of the T4 terrace of the Youjiang River in the Bose Basin were deposited about 800,000 years ago. The artifacts discovered in the same levels should be contemporaneous with the tektites. The tektites are fresh with sharp angles showing no reworking process and were found in situ associated with artifacts (Fig. 2). The timing of these layers may be further refined to 790 ka, if the recent dating of Australasian tektite to 788.1 ± 2.8 ka (Jourdan et al., 2019) is taken into account. The dating results of the tektites in our study can be refined in the near future via $^{40}Ar/^{39}Ar$ analysis by temperature increments to obtain: (1) plateau ages and (2) the corresponding isochron ages, rather than from series of TF, to eliminate the possible contributions of argon gas contamination at the beginning of heating.

Our new data solidly establish the existence of bifaces at around 800 ka on terrace T4 of Bose, which is similar to the date for Yunxian (de Lumley and Li, 2008) for bifaces discovered on the surface (936–800 ka; Wang et al., 2014; Wang and Bae, 2015). Nonetheless, the origin of bifaces in China remains obscure. For the sites of Bose, South China, choppers are generally dominant, but bifaces, picks, and some unifaces are also present, often on thick cobbles but also on flat pebbles or large flakes (Huang et al., 2012; Kuman et al., 2014; Wang et al., 2014; Li et al., 2014, 2016). There are very few atypical cleavers. Biface ratios are low (less than 5% except, for instance, at Fengshudao at 31%) and differ somewhat between localities (Zhang et al., 2010; Wang et al., 2012, 2014). Biface technology indicates cruder bifacial tools (minimally shaped, pick-like) than Acheulean tools; however, some tools share common features with the earliest African assemblages (Gao and Guan, 2018). The debate surrounding the origin of the bifaces in China is thus still open, as shown by recent articles, with some researchers considering the Chinese sites as Acheulean (i.e., Kuman et al., 2014; Li et al., 2014; 2015; Lei et al., 2020), whereas others considering them to have originated in situ, i.e., local onset (i.e., Wang et al., 2014). New findings in the North of China show the complexity of Chinese records, where diversified environments and the available local raw materials required adaptation (Li et al., 2017~~;~~; Li et al., (Li et al., 2017 and Li et al., 2018 are not the same authors, see references, thanks) 2018; Sherwood et al., 2018; Yang et al., 2020).

The lithic series of Nalai is composed of a low ratio of bifaces, and for most of them, a small portion of the tool is shaped. Shaping is often partial, on thick cobbles. The bifacially worked tools constitute a very small proportion of a much larger set of choppers and chopping tools. The bifacially worked tools do not have the classic length, breadth, and thickness proportions compared with African Acheulean tools. The mean breadth of these tools is much greater than for any known Western series, wherein the limit is usually about 100 mm. This may not be classic Acheulean, but it reflects a similar level of skill and complexity.

China represents a world apart from Southeast Asia, India, and Africa (Hou et al., 2000; Wang and Bae, 2015), but some similarities can be observed between China and early sites in the North of Thailand (Moncel et al., 2018). The pebble tool assemblages from the Southeast Asian Mainland appear to mark continuity with the Chinese world and a rupture with Southeast Asian islands. The diversity of the hominins attributed to *Homo erectus* associated with bifacial tools could explain the diversity of the technological strategies and morphological results (~~Li and Etler, 1992~~ Li and Etler, 1992; Vialet et al., 2010; Zhu et al., 2015).

The peopling of India is considered to have followed coastal routes from the west, in which case, bifacial technology would stem from the sphere of the Levant (Pappu et al., 2011; Kuman et al., 2016; Lei et al., 2020). This may or may not be the case for China, which was perhaps more isolated from the rest of Eurasia or never affected by the Acheulean dispersal as in the Levant, India, or South Asia. Accumulative behavioral processes influenced by local backgrounds owing to slow dispersals of populations or ideas through Asia could explain the specificity of Chinese heavy-duty tools, as in Western Europe.

Acknowledgments

We thank Wei Liao (Guangxi Museum Nationalities) and Fred Jourdan for helpful discussions. We also thank the co-Editor of *Journal of Human Evolution* A.B. Taylor, C. Koeberl, and one anonymous reviewer for constructive review and helpful comments. Louise Byrne is acknowledged for English improvements of the manuscript. This work was carried out with partial financial support from CEPAM-CNRS. There is no conflict of interest.

Appendix A. Supplementary Online Material

Supplementary online material to this article can be found online at https://doi.org/10.1016/j.jhevol.2021.102953.

Uncited references

~~Koppers (2002).~~

References

Bar-Yosef O. and Goren-Inbar N., The lithic assemblages of 'Ubeidiya. A Lower Palaeolithic site in the Jordan Valley, *Qedem* **34**, 1993.

Beyene Y., Katoh S., WoldeGabriel G., Hart W.K., Uto K., Sudo M., Kondo M., Hyodo M., Renne P.R., Suwa G. and Asfaw B., The characteristics and chronology of the earliest Acheulean at Konso, Ethiopia, *Proc. Natl. Acad. Sci.*

USA **110**, 2013, 1584–1591.

Cavosie A.J., Timms N.E., Erickson T.M. and Koeberl C., New clues from earth's most elusive impact crater: Evidence of reidite in Australasian tektites from Thailand, *Geology* **46**, 2017~~7~~8, 203–206, https://doi.org/10.1130/G39711.1.

de la Torre I., The Early Stone Age lithic assemblages of Gadeb (Ethiopia) and the developed Oldowan/early Acheulean in East Africa, *J. Hum. Evol.* **60**, 2011, 768–812.

de la Torre I., The origins of the Acheulean: Past and present perspectives on a major transition in human evolution, *Philos. T. R. Soc. B* **371**, 2016, 20150245.

de la Torre I., Mora R. and Martinez-Moreno J., The early Acheulean in Peninj (Lake Natron, Tanzania), *J. Anthropol. Archaeol.* **27**, 2008, 244–264.

de la Torre I. and Mora R., Technological behaviour in the early Acheulean of EF-HR (Olduvai Gorge, Tanzania), *J. Hum. Evol.* **120**, 2018, 329–377.

de Lumley H. and Li T., Le site de l'Homme de Yunxian. Quyuanhekou, Qingqu, Yunxian, Province du Hubei, 2008, CNRS éditions et éditions Recherche sur les Civilisations, 587.

Feng X., Qi Y., Li Q., Ma X. and Liu K., The industry of the Lower Paleolithic site of Baigu, Bose Basin, Guangxi Zhuang autonome Province, PR China, *L'Anthropologie* **122**, 2018, 14–32.

Folco L., Bigazzi G., D'Orazio M. and Balestrieri M.L., Fission track age of Transantarctic Mountain microtektites, *Geochem. Cosmochim. Acta* **75**, 2011, 2356–2360.

Folco L., Glass B.P., D'Orazio M. and Rochette P., A common volatilization trend in Transantarctic Mountain and Australasian microtektites: Implications for their formation model and parent crater location, *Earth Planet Sc Lett.* **293**, 2010, 135–139, https://doi.org/10.1016/j.epsl.2010.02.037.

Gao X., Characteristics and significance of Paleolithic handaxes from China, *Acta Anthropol. Sin.* **31**, 2012, 97–112.

Gao X. and Guan Y., Handaxes and the Pick-Chopper industry of Pleistocene China, *Quat. Int.* **480**, 2018, 132–140.

Glass B.P. and Koeberl C., Australasian microtektites and associated impact ejecta in the South China Sea and the Middle Pleistocene supereruption of Toba, *Meteoritics Planet Sci.* **1**, 2006, 305–326, https://doi.org/10.1111/j.1945-5100.2006.tb00211.x.

Goren-Inbar N., Alperson-Afil N., Sharon G. and Herzlinger G., The Acheulian Site of Gesher Benot Ya ʻaqov Volume IV. The Lithic Assemblages, 2018, Springer; Cham.

Guan Y., Xu X., Kuman K., Wu H., Zhou Z. and Gao X., The absence of Acheulean: Qiliting Mode 1 site and the Mode 1 occupations in southeast China, *Quat. Int.* **480**, 2018, 152–165.

Guo S.L., Huang W., Hao X.-H. and Chen B.L., Fission Track dating of ancient man site in Baise, China, and its significances in space research, paleomagnetism and stratigraphy, *Radiat. Meas.* **28**, 1997, 565–570, https://doi.org/10.1016/S1350-4487(97)00140-6.

Heide K., Heide G. and Kloess G., Glass chemistry of tektites, *Planet. Space Sci.* **49**, 2001, 839–844.

Hou Y., Potts R., Baoyin Y., Zhengtang G., Deino A., Wang W., Clark J., Xie G. and Huang W., Mid-Pleistocene Acheulean-like stone technology of the Bose Basin, South China, *Science* **287**, 2000, 1622–1626, https://doi.org/10.1126/science.287.5458.1622.

Huang S., Wang W., Bae C.J., Xu G. and Liu K., Recent Paleolithic field investigations in Bose Basin (Guangxi, China), *Quat. Int.* **281**, 2012, 5–9.

Jourdan F., Verati C. and Féraud G., Intercalibration of the HB3gr $^{40}Ar/^{39}Ar$ dating standard, *Chem. Geol.* **231**, 2006, 177–189.

Jourdan F., Mark D.F. and Verati C., Advances in dating: From archaeology to planetary sciences – introduction, *Geological Society* **378**, 2014, 1–8, London, Special Publications.

Jourdan F., Nomade S., Wingate M.T.D., Eroglu E. and Deino A., Ultraprecise age and formation temperature of the Australian tektites constrained by $^{40}Ar/^{39}Ar$ analyses, *Meteoritics Planet Sci.* **54**, 2019, 2573–2591, https://doi.org/10.1111/maps.13305.

Koeberl C., The geochemistry of tektites: An overview, *Tectonophysics* **171**, 1990, 405–422.

Koeberl C. and Glass B.P., Tektites and the age paradox in Mid-Pleistocene China, *Science* **289**, 2000, 507a.

Koppers A.A.P., ArArCALC software for $^{40}Ar/^{39}Ar$ age calculations, *Comput. Geosci.* **28**, 2002, 605–619.

Kuiper K.F., Deino A., Hilgen F.J., Krijgsman W., Renne P.R. and Wijbrans J.R., Synchronizing rocks clocks of earth history, *Science* **320**, 2008, 500–504, https://doi.org/10.1126/science.289.5479.507a.

Kuman K., Li C. and Li H., Large cutting tools in the Danjiangkou Reservoir Region, central China, *J. Hum. Evol.* **76**, 2014, 129–153.

Kuman K., Li H. and Li C., Large cutting tools from the Danjiangkou Reservoir Region, central China: Comparisons and contrasts with western and South Asian Acheulean, *Quat. Int.* **400**, 2016, 58–64.

Langbroek M., Do tektites really date the bifaces from the Bose (Baise) Basin, Guangxi, southern China?, *J. Hum. Evol.* **80**, 2015, 175–178.

Lee J.-Y., Marti K., Severinghaus J.P., Kawamura K., Yoo H.-S., Lee J.B. and Kim J.S., A redetermination of the isotopic abundances of atmospheric Ar, *Geochem. Cosmochim. Acta* **70**, 2006, 4507–4512, https://doi.org/10.1016/j.gca.2006.06.1563.

Lei L., Lotter M.G., Li D., Kuman K. and Li H., Refining the understanding of large cutting tool technology in the Baise Basin, South China, *Lithic Technol.* 2020, 1–17, https://doi.org/10.1080/01977261.2020.1841958.

Lepre C.L., Roche H., Kent D.V., Harmand S., Quinn R.L., Brugal J.-P., Texier P.-J., Lenoble A. and Feibel C.S., An earlier origin for the Acheulian, *Nature* **477**, 2011, 82–85.

Liao W., Li J., Li D., Huang Z., Luo Z., Tiang F. and Wang W., Paleolithic stone artifacts and tektite from the Nalai site at Tianyang County, Guangxi Province, *Quat. Sci.* **37**, 2017, 765–777, https://doi.org/10.11928/j.issn.1001 7410.2017.04.09.

Li H., Li C.R., Kuman K., Cheng J., Yao H.T. and Li Z., The Middle Pleistocene handaxe site of Shuangshu in the Danjiangkou Reservoir region, central China, *J. Archaeol. Sci.* **52**, 2014, 391–409.

Li H., Kuman K. and Li C., Quantifying the reduction intensity of handaxes with 3D technology: A pilot study on handaxes in the Danjiangkou Reservoir region, central China, *PLoS One* **10** (9), 2015, e0135613.

Li H., Kuman K. and Li C., The symmetry of handaxes from the Danjiangkou Reservoir Region (central China): A methodological consideration, *Quat. Int.* **400**, 2016, 65–72.

Li H., Kuman K. and Li C., What is currently (un) known about the Chinese Acheulean, with implications for hypotheses on the earlier dispersal of hominids, *C. R. Palevol* **17**, 2018, 120–130.

Li T. and Etler D.A., New Middle Pleistocene hominid crania from Yunxian in China, *Nature* **357**, 1992, 405–407.

Li X., Ao H., Dekkers M.J., Roberts A.P., Zhang P., Lin S., Huang W., Hou Y., Zhang W. and An Z., Early Pleistocene occurrence of Acheulian technology in North China, *Quat. Sci. Rev.* **156**, 2017, 12–22.

Ludwig K.R., User's manual for Isoplot 3.0, *A Geochronological Toolkit for Microsoft Excel* 2003, Berkeley Geochronology Center, Special Publication No. 4.

Lycett S.J. and Bae C.J., The Movius Line controversy: The state of the debate, *World Archaeol.* **42**, 2010, 521–544.

Martinez-Navarro B., Belmaker M. and Bar-Yosef O., The Bovid assemblage (Bovidae, Mammalia) from the Early Pleistocene site of ‘Ubeidiya, Israel: Biochronological and paleoecological implications for the fossil and lithic bearing strata, *Quat. Int.* **267**, 2012, 78–97.

Mizera J., Randa Z. and Kamenik J., On a possible parent crater for Australasian tektites: geochemical, isotopic, geographical and other constraints, *Earth Sci. Rev.* **154**, 2016, 123–137, https://doi.org/10.1016/j.earscirev.2015.12.004.

Moncel M.-H., Despriée J., Voinchet P., Tissoux H., Moreno D., Bahain J.-J., Courcimault G. and Falguères C., Early evidence of Acheulean settlement in north-western Europe - la Noira site, a 700 000 year-old occupation in the center of France, *PLoS One* **8** (11), 2013, e75529.

Moncel M.-H., Arzarello M., Boëda E., Bonilauri T., Chevrier B., Gaillard C., Forestier H., Yinghua L., Sémah F. and Zeitoun V., Assemblages with bifacial tools in Eurasia (second part). What is going on in the East? Data from India, Eastern Asia and Southeast Asia, *C. R. Palevol* **17**, 2018, 61–76.

Moncel M.-H. and Ashton N., From 800 to 500 ka in Europe. The oldest evidence of Acheuleans in their technological, chronological and geographical framework, In: Mussi M. and Gallotti R., (Eds.), *The Emergence of the Acheulean in East Africa,* 2018, Springer Edition; Cham, 215–235.

Nomade S., Renne P.R., Vogel N., Deino A.L., Sharp W.D., Becker T.A., Jaouni A.R. and Mundil R., Alder Creek sanidine (ACs-2): a Quaternary 40Ar/39Ar dating standard tied to the Cobb Mountain geomagnetic event, *Chem. Geol.* **218**, 2005, 315–338, https://doi.org/10.1016/j.chemgeo.2005.01.005.

McDougall I., K/Ar and $^{40}Ar/^{39}Ar$ Isotopic Dating Techniques as Applied to Young Volcanic Rocks, Particularly Those Associated with Hominin Localities, In: 2nd Edition, *Treatise on Geochemistry* 2014, Elsevier Ltd; Amsterdam 1–15, https://doi.org/10.1016/B978-0-08-095975-7.01201-8.

Michel V., Shen G., Shen C.-C., Wu C.-C., Vérati C., Gallet S., Moncel M.-H., Combier J., Khatib S. and Manetti M., Application of U/Th and $^{40}Ar/^{39}Ar$ dating to Orgnac 3, a Late Acheulean and Early Middle Palaeolithic site in Ardèche, France, *PLoS One* **8** (12), 2013, e82394 https://doi:10.1371/journal.pone.0082394 http://www.plosone.org/article/info%3Adoi%2F10.1371%2Fjournal.pone.0082394.

Movius H.L., Early man and Pleistocene stratigraphy in southern and eastern Asia. Harvard University, Peabody Museum papers 19(3), 1944, Peabody Museum; Cambridge, MA.

Pappu S., Gunnell Y., Akhilesh K., Braucher R., Taieb M., Demory F. and Thouveny N., Early Pleistocene presence of Acheulian hominins in South India, *Science* **331**, 2011, 1596–1599.

Potts R., Huang W., Hou Y., Deino A., Baoyin Y., Zhengtang G. and Clark J., Tektites and the age paradox in Mid-Pleistocene China. Response, *Science* **289**, 2000, 507a, https://doi.org/10.1126/science.289.5479.505n.

Renne P.R., Sharp Z.D. and Heizler M.T., Cl-derived argon isotope production in the CLICIT facility of OSTR reactor and the effects of the Cl-correction in $^{40}Ar/^{39}Ar$ geochronology, *Chem. Geol.* **255**, 2008, 463–466.

Renne P.R., Deino A.L., Hames W.E., Heizler M.T., Hemming S.R., Kopper A.A.P., Mark D.F., Morgan L.E., Phillips D., Singer B.S., Turrin B.D., Villa I.M., Villeneuve M. and Wijbrans J.R., Data reporting norms for $^{40}Ar/^{39}Ar$ geochronology, *Quat. Geochronol.* **4**, 2009, 346–352, https://doi.org/10.1016/j.quageo.2009.06.005.

Rochette P., Braucher R., Folco L., Horng C.S., Aumaître G., Bourlès D.L. and Keddadouche K., ^{10}Be in Australasian microtektites compared to tektites: size and geographic controls, *Geology* **46**, 2018, 803–806, https://doi.org/10.1130/G45038.1.

Schwarz W.H., Trieloff M., Bollinger K., Gantert N., Fernandes V.A., Meyer H.P., Povenmire H., Jessberger E.K., Guglielmino M. and Koeberl C., Coeval ages of Australasian, Central American and Western Canadian tektites revea multiple impacts 790 ka ago, *Geochem. Cosmochim. Acta* **178**, 2016, 307–319, https://doi.org/10.1016/j.gca.2015.12.037.

Semaw S., Rogers M.J. and Stout D., The Oldowan-Acheulean transition: Is there a “Developed Oldowan” Artifact Tradition?, In: Camps M. and Chauhan P., (Eds.), *Sourcebook of Paleolithic Transitions,* 2009, Springer Editions; New York, 173–193, https://doi.org/10.1007/978-0-387-76487-0_10.

Sharon G., Acheulian Large Flake Industries: Technology, Chronology, and Significance, 2007, BAR International Series, 1701. Archaeopress; Oxford, UK.

Sherwood N.L., Li H., Kuman K. and Li C., Lithic raw material quality of Middle Pleistocene artifacts from the Han River, Danjiangkou Reservoir Region, central China, *Quat. Int.* **480**, 2018, 141–151.

Sieh K., Herrin J., Jicha B., Angel D.S., Moore J.D.P., Banerjee P., Wiwegwin W., Sihavong V., Singer B., CHualaowanich T. and Charusin P., Australasian impact crater buried under the Bolaven volcanic field, *Southern Laos. Proc. Natl. Acad. Sci. USA* **117**, 2020, 1346–1353.

Steiger R.H. and Jäger E., Subcommission on geochronology: Convention on the use of decay constants in geo- and cosmochronology, *Earth Planet Sci. Lett.* **36**, 1977, 359–362, https://doi.org/10.1016/0012-821X(77)90060-7.

Tetley N. and McDougall I., Thermal neutron interferences in the $^{40}Ar/^{39}Ar$ dating technique, *J. Geophys. Res.* **85**, 1980, 7201–7205.

Vallverdu J., Saladié P.S., Rosas A., Huguet R., Caceres I., Mosquera M., Garcia-Taberno A., Estalrrich A., Lozana-Fernandez I., Pineda-Alcala A., Carrancho A., Villalain J.J., Bourlès D., Braucher R., Lebatard E., Vilalta J., Esteban-Nadal M., Bennasar M.L., Bastir M., Lopez-Polin L., Ollé A., Vergés J.M., Ros-Montoya S., Martinez-Navarro B., Garcia A., Martinell J., Exposito I., Burjachs F., Agusti J. and Carbonell E., Age and date for early arrival of the Acheulian in Europe (Barranc de la Boella, la Canonja, Spain), *PLoS One* **9**, 2014, e103634.

Vialet A., Guipert G., Jianing H., Xiaobo F., Zune L., Youping W., Tianyuan L., de Lumley M.-A. and de Lumley H., *Homo erectus* from the Yunxian and Nankin Chinese sites: Anthropological insights using 3D virtual imaging techniques, *C. R. Palevol* **9**, 2010, 331–339.

Voinchet P., Moreno D., Bahain J.-J., Tissoux H., Tombret O., Falguères, Moncel M.-H., Schreve D., Candy I., Antoine P., Ashton N., Beamish M., Cliquet D., Despriée J., Lewis S., Limondin-Lozouet N., Locht J.-L., Parfitt S. and Pope M.,

New chronological data (ESR and ESR/U-series) for the earliest Acheulean sites of north-western Europe, *J. Quat. Sci.* **30**, 2015, 610–622.

Wang W., Lycett S.J., von Cramon-Taubadel N., Jin J.J. and Bae C.J., Comparison of handaxes from Bose Basin (China) and the western Acheulean indicates convergence of form, not cognitive differences, *PLoS One* **7** (4), 2012 e35804.

Wang W., Bae C.J., Huang S., Huang X., Tian F., Mo J., Huang C., Xie S. and Li D., Middle Pleistocene bifaces from Fengshudao (Bose Basin, Guangxi, China), *J. Hum. Evol.* **69**, 2014, 110–122.

Wang W. and Bae C.J., How old are the Bose (Baise) Basin (Guangxi, southern China) bifaces? the Australasian tektites question revisited, *J. Hum. Evol.* **80**, 2015, 171–174.

Xie G.-M. and Bodin E., Les industries paléolithiques du Bassin de Bose (Chine du Sud), *L'Anthropologie* **111**, 2007, 182–206, https://doi.org/10.1016/j.anthro.2007.03.002.

Xu G., Wang W., Bae C.J., Huang S. and Mo Z., Spatial distribution of Paleolithic sites in Bose Basin, Guangxi, China, *Quat. Int.* **281**, 2012, 10–13.

Yang S.-X., Yue J.-P., Zhou X., Strorozum M., Huan F.-X., Deng C.-L. and Petraglia M.D., Hominin site distributions and behaviors across the Mid-Pleistocene climate transition in China, *Quat. Sci. Rev.* **248**, 2020, 106614.

Zhang P., Huang W. and Wang W., Acheulean handaxes from Fengshudao, Bose sites of South China, *Quat. Int.* **223–224**, 2010, 440–443, https://doi.org/10.1016/j.quaint.2009.07.009.

Zhu Z.-Y., Dennell R., Huang W.-W., Wu Y., Rao Z.-G., Qiu S.-F., Xie J.-B., Liu L., Fu S.-Q., Han J.-W., Zhou H.-Y., Ou Yang T.-P. and Li H.-M., New dating of the *Homo erectus* cranium from Lantian (Gongwangling), China, *J. Hum. Evo* **78**, 2015, 144–157.

Appendix A. Supplementary Online Material (First $^{40}Ar/^{39}Ar$ analyses of Australasian tektites in close association with bifacially worked artifacts at Nalai site in Bose Basin, South China: the question of the early Chinese Acheulean) (First $^{40}Ar/^{39}Ar$ analyses of Australasian tektites in close association with bifacially worked artifacts at Nalai site in Bose Basin, South China: The question of the early Chinese Acheulean) (Please change the title as in the Main text :)

The following is the Supplementary online material to this article:

Multimedia Component 1

Multimedia component 1

alt-text: Multimedia component 1